Extracting H_0 and r_d in Pacif Parametrization Models through Late-Time Dataset

Himanshu Chaudhary,[1,*] Shibesh Kumar Jas Pacif,[1,†] G. Mustafa,[2,3,‡] Amine Bouali,[4,§] and Faisal Javed[2,¶]

[1]*Pacif Institute of Cosmology and Selfology (PICS), Sagara, Sambalpur 768224, Odisha, India*
[2]*Department of Physics, Zhejiang Normal University, Jinhua 321004, Peoples Republic of China*
[3]*New Uzbekistan University, Mustaqillik ave. 54, 100007 Tashkent, Uzbekistan*
[4]*Laboratory of Physics of Matter and Radiation, Mohammed I University, BP 717, Oujda, Morocco*

This study examines five models derived from the Pacif parametrization scheme of the Hubble parameter (H), yielding various linear to quintic forms of the deceleration parameter (DP). Our goal is to explore the impact of these DP variations on late-time evolution and their potential to alleviate cosmological tensions. To enhance model constraints, we introduce non-diagonal elements into the covariance matrix to better capture statistical properties by simulating data point correlations. We also test the sensitivity of H_0 and r_d to the Pacif parametrization scheme, treating the sound horizon r_d as a free parameter to avoid imposing a CMB prior. This allows late-time data to constrain r_d alongside other cosmological parameters, incorporating recent Baryon Acoustic Oscillations (BAO) measurements and Hubble data from Cosmic Chronometers Methods, Type Ia Supernovae (SNIa), Gamma-Ray Bursts (GRBs), and Quasars over a redshift range of $0.106 < z < 2.33$. Our analysis provides optimal fit values for H_0 and r_d, showing notable consistency with Planck CMB data. By using the Akaike information criterion, we analyze the models and conclude that all models have good agreement with the most recent observations.

I. INTRODUCTION

The enigma of late-time cosmic acceleration (LTCA) stands as an enthralling mystery in the realms of contemporary astrophysics and cosmology [1]. Across recent decades, a cascade of observational evidence has consistently pointed to an unexpected acceleration in the expansive dance of the Universe, thereby challenging the very bedrock of our comprehension regarding the fundamental forces and constituents steering its majestic dynamics. The monumental revelation of the accelerated expansion, initially discerned from the distant glimmer of supernovae in the late 1990s [2–12], has etched itself as a transformative cornerstone in the grand tapestry of cosmological exploration. Subsequent observations, spanning the CMBR, sprawling large-scale structure surveys, and the subtle echoes of baryon acoustic oscillations, have relentlessly affirmed [3, 13–15] the reality of late-time cosmic acceleration, prodding at the edges of established cosmological models and setting forth an urgent quest for novel theoretical frameworks. In the intricate quest to elucidate the observed cosmic acceleration, a pantheon of hypotheses has emerged, unfurling possibilities that include the modification of gravity theory, the introduction of additional terms into the revered Einstein Field Equations (EFEs), and alternative conceptualizations. Notably, the compelling concept of dark energy, an ethereal force draped in highly negative pressure, has ascended to the forefront of contemporary cosmology. The riddles concealed within the labyrinth of dark energy's nature, grounded in the meticulous observations facilitated by cutting-edge astronomical instruments and space-based missions, confront the established principles guiding cosmic evolution, beckoning scientists to embark on a profound exploration of its elusive essence [16, 17].

Some applications of the so-called Cosmography with gamma-ray burst (GRB) were presented by Izzo et al. [18] Specifically, an attempt is made to use the luminosity distance discovered through cosmographic study to calibrate the Amati relation. They so examined the potential for employing GRBs as potential estimators for the cosmological parameters and using only a sample of GRB data, they were able to generate a good estimate of the cosmic density parameters as preliminary results [18]. Aviles et al. [19] employed cosmography to demonstrate limitations on the Universe's kinematics without proposing an underlying theoretical model. When the Padé expansion is required to be positive, it is discovered that the Padé convergence radii are larger than the standard Taylor convergence radii. This implies a lower limit on the Universe's acceleration [20]. The research on reducing systematics, overcoming the degeneracy between cosmological coefficients, handling divergences, and other relevant topics is specifically

* himanshuch1729@gmail.com
† shibesh.math@gmail.com
‡ gmustafa3828@gmail.com
§ a1.bouali@ump.ac.ma
¶ faisaljaved.math@gmail.com

presented in [21, 22]. The statefinder parameters, as determined by standard cosmography described in [23], turn out to be biased and poorly calculated when using simulated supernova catalogs. In order to address the issue of error propagation during statistical analysis, the bounds of standard cosmography are altered in [24]. The Padé approximations were examined by Capozziello et al. [25] up to the fifth order, and these series were compared with the corresponding variables of the same orders. Further, the GRBs are investigated by using the Padé approximations and also employed the Beziér polynomials for the correlations and heal the circularity problem in [26, 27] and Ref. [28] provides a model-independent reconstruction of the cosmological accelerated-decelerated phase. Understanding the transition and equivalency epochs between dark energy and matter can help us understand dark energy's properties at redshifts higher than the current one. Although the ΛCDM paradigm continues to offer the best background model, Alfano et al. [29] shown that the constraints on dark energy evolution cannot exclude a little evolution at intermediate redshifts. The direct comparison between the ΛCDM and wCDM models, as well as the Chevallier-Polarski-Linder parametrization, was investigated and reported by Luongoa and Muccino [30].

The unraveling of dark energy's enigma entails meticulous scrutiny of various theoretical candidates [31, 32]. The widely pondered cosmological constant standing as the most favourable candidate of DE with constant energy density. However, it encounters formidable challenges, notably encapsulated in the enigmatic "cosmological constant problem." Conversely, quintessence fields introduce dynamic scalar entities that gracefully evolve through the cosmic epochs, leaving an indelible imprint on the energy density and expansion rate of the Universe. Parallelly, modified gravity theories, exemplified by the intriguing f(R) gravity, propose alterations to Einstein's venerable general relativity as potential conduits explaining cosmic acceleration. Introducing an additional layer of complexity into the Einstein Field Equations introduces challenges in uncovering exact solutions, steering scientists towards numerical avenues like dynamical system analysis and pragmatic, model-independent approaches [33]. These model-independent forays, often employing various cosmological parametrization schemes [34, 35], emerge as elegant mathematical tools, providing nuanced solutions to the intricate EFEs. The multifaceted nature of dark energy mandates a flexible approach to its characterization, and cosmological parametrization schemes emerge as powerful instruments embodying this adaptability. These schemes, adept at expressing the equation of state (EoS) of dark energy by relating its pressure and energy density, rely on parameters encapsulating the underlying physics. Through the prism of parametrization, researchers can traverse a diverse landscape of dark energy behaviors without tethering themselves to a specific theoretical framework.

Dealing with the various datasets in constraining cosmological models also results in some issues. The persistent discrepancies and conflicts observed between different measurements or predictions within the field are quite evident. These tensions, often arising from diverse observational methods or data sets, challenge the harmonious narrative sought by cosmologists in understanding the fundamental aspects of the Universe. One notable example is the Hubble constant tension, where measurements of the rate of the Universe's expansion derived from early and late-time observations yield conflicting results [36, 37]. This tension hints at potential gaps or unknown phenomena in our current understanding of cosmic evolution. The existence of such tensions underscores the need for a comprehensive and unified framework in cosmology, compelling scientists to reevaluate assumptions, refine models, and embark on a collective effort to reconcile divergent aspects of the cosmos. Researchers have extensively discussed and analyzed the parametrization of the deceleration parameter, Hubble parameter, and other geometrical and physical parameters in the literature. A brief summary of this work can be found [38–62]. In this work, we are addressing the H_0 and r_d tensions in some dark energy models resulting from Pacif parametrization scheme.

The paper is structured as follows: In Section II, we delve into the background of the Pacif Parametrization Scheme and the Models in the standard theory of gravity. Moving on to Section III, we focus on the methodology employed for constraining the crucial parameters of both ΛCDM and the model obtained through the Pacif parameterization scheme, utilizing various datasets. Our study's outcomes are detailed in Section IV, where we present the results. Finally, in Section V, we conclude the paper, offering discussions on the implications and significance of our findings.

II. PACIF PARAMETRIZATION SCHEME AND THE MODELS

If we consider the homogeneous and isotropic spacetime with a flat spatial section, then the dark energy can be characterized by a large-scale scalar field ϕ that is predominantly governed by either potential energy or nearly constant potential energy, thereby violating positive energy constraints. Such a form of *matter* exhibits an energy-stress tensor represented as $T_{ij}^{\rm DE} = (\rho_\phi + p_\phi)U_iU_j + p_\phi\, g_{ij}$ and an equation of state expressed as $p_\phi = w_\phi\rho_\phi$, where the parameter w_ϕ is generally a function of time. This framework offers several potential candidates for dark energy, contingent upon the dynamic behavior of the field ϕ and its associated potential energy. Among these candidates, the most straightforward and widely favored one, as supported by cosmological observations, is Einstein's cosmological constant Λ, where w_ϕ attains the constant value of -1, indicative of a scalar field dominated by potential energy. The incorporation of dark energy into Einstein's theory involves $T_{ij}^{\rm total}$, where $T_{ij}^{\rm total} = T_{ij}^{\rm M} + T_{ij}^{\rm DE} = (\rho_{\rm t} + p_{\rm t})U_iU_j + p_{\rm t}\, g_{ij}$. Here, $\rho_{\rm t} = \rho + \rho_\phi$ and $p_{\rm t} = p + p_\phi$. Consequently, field equations are modified as follows:

$$8\pi G\rho_{\rm t} = 3\frac{\dot{a}^2}{a^2}, \tag{1}$$

$$8\pi G p_{\rm t} = -2\frac{\ddot{a}}{a} - \frac{\dot{a}^2}{a^2}. \tag{2}$$

The two observable parameters H (Hubble parameter) and q (deceleration parameter) defined respectively as $H = \dot{a}/a$ and $q = -a\,\ddot{a}/\dot{a}^2$ are two important geometrical parameters that describe the dynamics of the Universe and are also related by the relation

$$q = -1 + \frac{d}{dt}\left(\frac{1}{H}\right). \tag{3}$$

Solving the above set of equations is one of the tasks in cosmology. The system involves two independent equations and five unknowns: a, ρ, p, ρ_{de}, and p_{de} (or ω_{de}). Given the homogeneous distribution of matter at large scales in the Universe, a common practice is to consider the Universe to be filled with perfect fluid and so using the barotropic equation of state $p = \omega\rho$, where ω takes values within the range [0, 1]. This equation of state describes various types of matter sources in the Universe, depending on discrete or dynamic values of the equation of state parameter ω. Another crucial constraint arises from considering the equation of state of dark energy (ω_{de} = constant or a function of time t or a function of scale factor a or a function of redshift z), known as the parametrization of dark energy equation of state. These four equations collectively elucidate the cosmological dynamics of the Universe, expressing geometric parameters (Hubble parameter H, deceleration parameter q, jerk parameter j, snap parameter s, lerk parameter l etc.) or the physical parameters (densities ρ, ρ_{de}, pressures p, p_{de}, EoS parameter ω_{de}, density parameter Ω_i, etc.) as functions of either scale factor a or redshift z.

In the realm of solving Einstein field equations (EFEs), a critical analysis reveals two key aspects. Firstly, the parametrization of geometrical parameters a, H, q, and j provides time-dependent functions for all cosmological parameters, commonly referred to as a "model-independent way" study or cosmological parametrization. This method aims to find exact solutions, discussing the expansion dynamics of the Universe and offering time evolution insights into physical parameters such as ρ, p, ρ_{de}, p_{de} (or ω_{de}). Notably, this approach is advantageous in elucidating the cosmic history of the Universe, addressing issues such as the initial singularity problem and cosmological constant problem, and theoretically explaining the late-time acceleration conundrum. Secondly, the parametrization of physical parameters is often employed to delve into the broader physical aspects of the Universe, encompassing thermodynamics, structure formation, nucleosynthesis, and more. Both parametrization schemes involve arbitrary constants, termed as "*model parameters*," which are constrained through observational datasets. The primary objective here is to attain an exact solution of the Einstein field equations within standard general relativity theory, employing a straightforward parametrization of the Hubble parameter H to discuss the reconstructed cosmic evolution.

In the standard approximation, the scale factor can be expanded in the Taylor series around the present time t_0 (which is the current age of the Universe also) and is the simple strategy adopted in cosmographical analysis. Here and afterward, a suffix 0 denotes the value of the parameter at present time t_0. The Taylor's series expansion can be written as:

$$\begin{aligned} a^{(n)} &= 1 + H_0(t-t_0) - \frac{1}{2!}q_0H_0^2(t-t_0)^2 + \frac{1}{3!}j_0H_0^3(t-t_0)^3 \\ &\quad + \frac{1}{4!}s_0H_0^4(t-t_0)^4 + \frac{1}{5!}l_0H_0^5(t-t_0)^5 + ... \end{aligned} \tag{4}$$

where $H(t) = \frac{1}{a}\frac{da}{dt}$ is the Hubble parameter measuring velocity, $q(t) = -\frac{1}{a}\frac{d^2a}{dt^2}\left[\frac{1}{a}\frac{da}{dt}\right]^{-2}$ is the deceleration

parameter measuring acceleration, $j(t) = \frac{1}{a}\frac{d^3a}{dt^3}\left[\frac{1}{a}\frac{da}{dt}\right]^{-3}$ jerk parameter measuring jerk, $s(t) = \frac{1}{a}\frac{d^4a}{dt^4}\left[\frac{1}{a}\frac{da}{dt}\right]^{-4}$ is the snap parameter and $l(t) = \frac{1}{a}\frac{d^5a}{dt^5}\left[\frac{1}{a}\frac{da}{dt}\right]^{-5}$ is the lerk parameter with its specific roles in describing the properties of the Universe. All of these parameters play significant roles in the cosmographic analysis of the Universe (specifically the H, q, and j) and distinguish various dark energy models. This discussion motivated us to consider a parametrization scheme that can provide a solution to the field equations and a deeper understanding of the cosmographic analysis. In view of this, consider the following form of $H(t)$ as also considered in the papers [33–35, 63, 64] :

$$H(t) = \frac{n}{t\,(m - t^p)} \tag{5}$$

For varying values of the parameter p (where p takes on values of 0, 1, 2, 3, ...), we have different functional forms of the Hubble parameter, which exhibit distinct functional forms of the deceleration parameter, progressing from lower to higher orders in cosmic time t. The constants m and n are characterized as the model parameters. Using the definition of the deceleration parameter (DP), we can find the explicit forms of $q(t)$ for different values of $p = 0, 1, 2, 3....$ We may classify the models as constant DP (CDP) model for $p = 0$, linearly varying DP (LVDP) for $p = 1$, Quadratically varying DP (QVDP) for $p = 2$, Cubic varying DP (CVDP) for $p = 3$, Quartic varying DP (QUADP) for $p = 4$, Quintic varying DP (QUIDP) for $p = 5$, and so on. In general, the form of $q(t)$ can be written as

$$q(t) = -1 + \frac{m}{n} - \frac{p+1}{n}t^p, \tag{6}$$

where the index p assumes values $0, 1, 2, 3, ...$ Further calculations provide the scale factor as

$$a(t) = C\left(\frac{t^p}{m - t^p}\right)^{\frac{n}{pm}} \tag{16}$$

Here, we aim to explore the cosmological implications of various orders of $q(t)$ functions during the later stages of the Universe's evolution and assess how these models align with observational data. We use the standard norms to establish the $t - z$ relationships for these models to write the Hubble parameter and deceleration parameter in terms of redshift z. We consider a $t = t_0$, $a = a_0$, where subscript 'a_0' denotes the present value of the scale factor and the cosmological redshift defined by the relation $1 + z = a_0/a$, then, we have,

$$H(z) = \frac{H_0}{\left(1 + \eta^{p\gamma}\right)^{\frac{p+1}{p}}\,(1+z)^{p\gamma}}\left[1 + \left\{\eta\,(1+z)\right\}^{p\gamma}\right]^{\frac{p+1}{p}} \tag{7}$$

and

$$q(z) = -1 + \gamma + \frac{(p+1)\gamma}{1 + \left[\eta(1+z)\right]^{p\gamma}}, \tag{8}$$

where η and γ are new model parameters related to m and n. We will constrain the model parameters η and γ in place of m and n. As we have already mentioned, different values of p render different models. Here, we will constrain five models: LVDP, QVDP, CVDP, QUADP, and QUIDP. The parametrization scheme utilized in our analysis produces diverse models characterized by deceleration parameter profiles showcasing an acceleration in the Universe's expansion rate during its later stages, as depicted in the following Fig. 1. Our main objective is to delve deeper into the implications of this observed cosmic acceleration on the Universe's overall evolution. The first model represents the well-known, power law cosmology with a constant deceleration parameter (CDP), which we will not further analyze. However, other models depicted as Linear, Quadratic, Cubic, Quartic, and Quintic varying deceleration parameter models, respectively, illustrate distinct behaviors during the late phases of evolution, as evident in Figure 1. All these models exhibit super acceleration, surpassing quintessence thresholds. Through meticulous examination, we aim to elucidate how this escalating acceleration may help resolve existing cosmological tensions or discrepancies within current models. By conducting comprehensive analysis and interpretation, we seek to glean valuable insights into the underlying mechanisms propelling this observed acceleration and its broader implications for our comprehension of the cosmos.

III. METHODOLOGY

In our analysis, we have chosen a subset of the latest Baryon Acoustic Oscillation (BAO) measurements sourced from various galaxy survey experiments. The predominant contributors to this subset are the Sloan Digital Sky Survey (SDSS) [65–70]. Additionally, we have incorporated data from the Dark Energy Survey (DES) [71], the Dark Energy Camera Legacy Survey (DECaLS) [72], and 6dFGS BAO [73]. In any analysis, understanding and properly accounting for correlations within the data are crucial for drawing accurate conclusions. This is especially true in cosmology, where

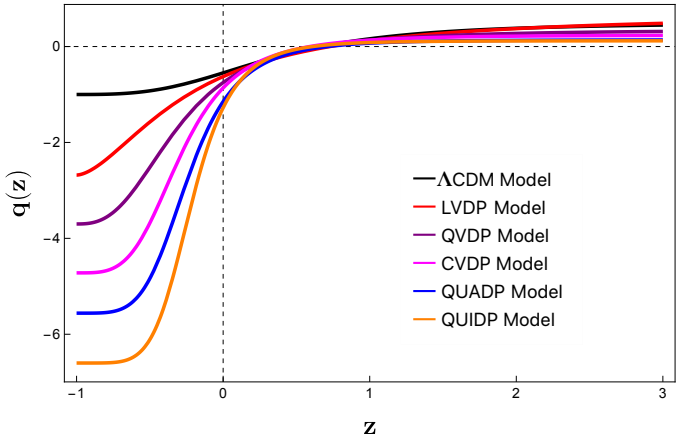

FIG. 1: The figure shows the evolution of the deceleration parameter for the considered models resulting from the Pacif parametrization scheme. We can interpret the higher acceleration rate for the described models in the late phase of the evolution.

precise measurements of observables like the Baryon Acoustic Oscillations (BAO) are essential for constraining cosmological models. In our analysis, we recognize the potential for correlations among selected data points, which could arise from various sources such as instrumental effects, observational biases, or underlying physical processes. To address this, we adopt a comprehensive approach outlined in [74], leveraging the concept of covariance matrices. The covariance matrix encapsulates the statistical relationships between different measurements in our dataset. In our case, we aim to estimate the covariance matrix for the BAO data, which informs us about the uncertainties and correlations associated with each measurement. However, accurately determining the covariance matrix is challenging, especially when dealing with diverse measurements from different observational surveys. To tackle this challenge, we employ a methodology inspired by [74]. Firstly, we acknowledge that while we intentionally curate a subset of data to mitigate highly correlated points, intrinsic correlations may still exist within our chosen data points. To simulate these correlations, we introduce non-diagonal elements into the covariance matrix while ensuring symmetry. This process involves randomly selecting pairs of data points and assigning non-diagonal elements with magnitudes determined by the product of the 1σ errors of the corresponding data points, scaled by a factor of 0.5. By incorporating these non-diagonal elements, we effectively model correlations between pairs of measurements. It's worth noting that this approach allows us to represent correlations within approximately 55% of the BAO dataset. While the specific locations of the non-diagonal elements are chosen randomly, the magnitudes are calculated to reflect the expected level of correlation between the corresponding data points. This enables us to more accurately capture the true statistical properties of the dataset and improve the robustness of our analysis. Our analysis employs Polychord, a nested sampling algorithm suitable for high-dimensional parameter spaces, along with the GetDist package for visualizing results [75, 76]. This combination of computational tools ensures efficient exploration of the parameter space and a clear presentation of the results. This algorithm facilitates the necessary calculations for our analysis. To determine the best-fit values for our cosmological model parameters, we augment the Baryon Acoustic Oscillations (BAO) dataset by incorporating thirty uncorrelated Hubble parameter measurements obtained through the cosmic chronometers (CC) method, detailed in [77–80]. The latest Pantheon sample data on Type Ia Supernovae [81] is also incorporated. Expanding our observational scope, we introduce 24 binned quasar distance modulus data from [82], a set of 162 Gamma-Ray Bursts (GRBs) as outlined in [83], and the recent Hubble constant measurement (R22) [84] as an additional prior.

IV. RESULTS

Fig 1 provides valuable insights into the behavior of the late Universe utilizing the Pacif parameterization scheme, which yields cosmological models featuring deceleration parameters of varying orders concerning cosmic time t. Notably, these models exhibit a compelling cosmological phase transition from an early decelerating phase to a late accelerating phase. The LVDP, QVDP, CVDP, QUADP, and QUIDP models all demonstrate this characteristic transition, eventually entering a phase of super acceleration ($q < -1$) in the distant future. This implication suggests that in these models, the Universe will undergo a "Big Rip" scenario, culminating in a singularity and the disintegration of all bound structures, including galaxies, stars, and even atoms. Consequently, Fig 2 illustrates posterior distributions for six cosmological models (ΛCDM, LVDP, QVDP, CVDP, QAVDP, and QIVDP) with and without the inclusion of a test random covariance matrix comprising fourteen components. Surprisingly, varying from null to fourteen components, the covariance matrix has minimal impact, closely resembling the uncorrelated dataset. These findings suggest a limited influence on model posterior distributions.

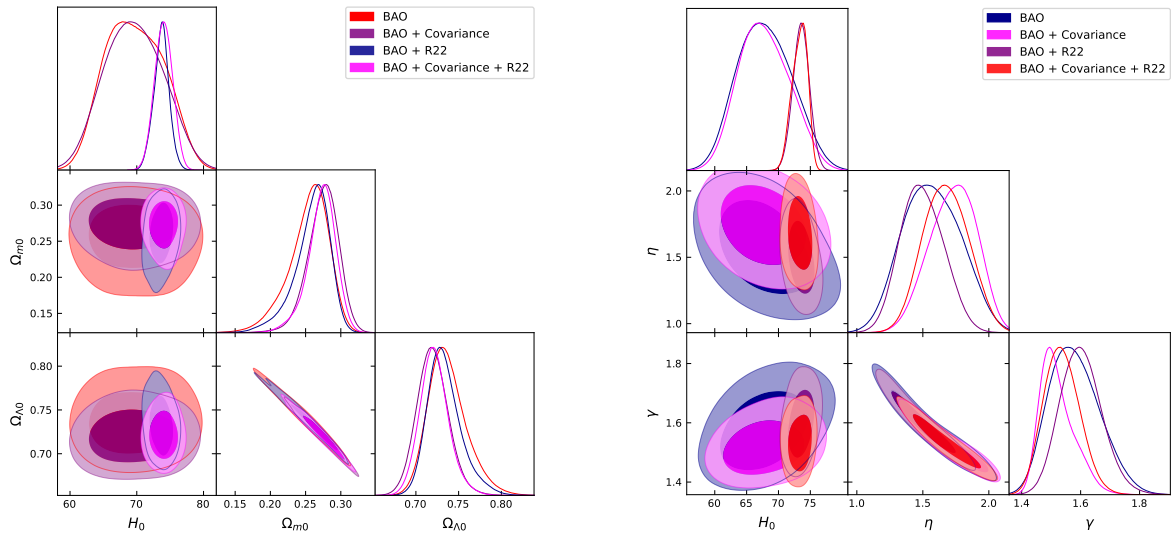

a) ΛCDM Model

b) LVDP Model

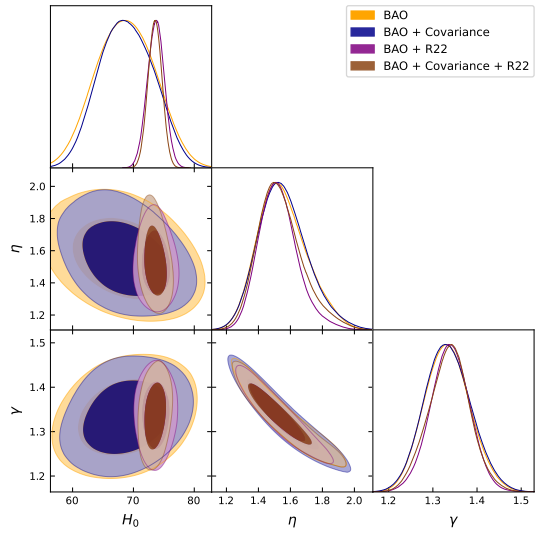

c) QVDP Model

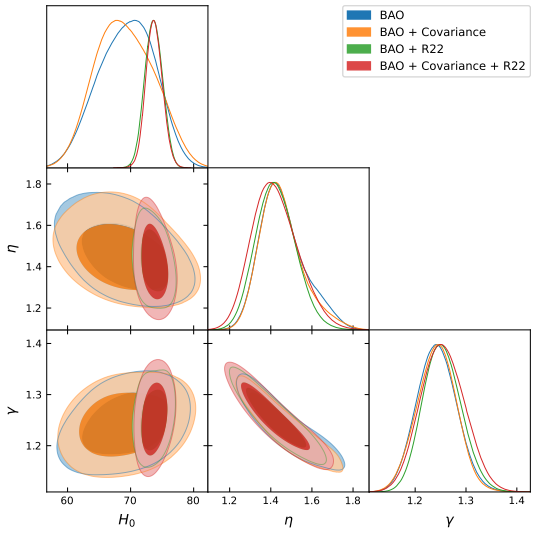

d) CVDP Model

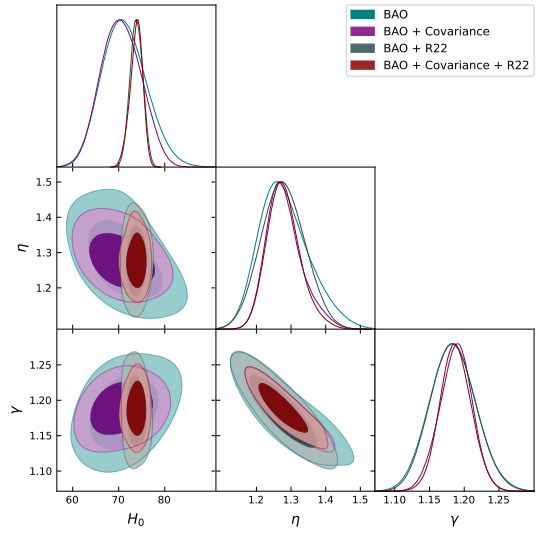

e) QUADP Model

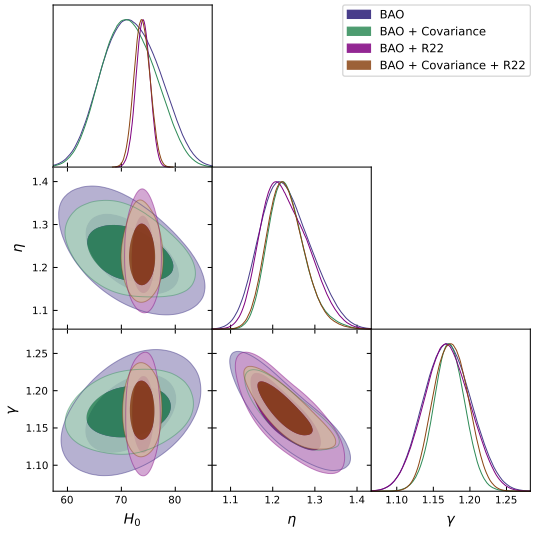

f) QUIDP Model

FIG. 2: The figure illustrates posterior distributions for ΛCDM, LVDP, QVDP, CVDP, QUADP, and QUIDP models using covariance matrix simulation. The impact of covariance matrices with up to fourteen components is negligible, closely resembling the uncorrelated dataset.

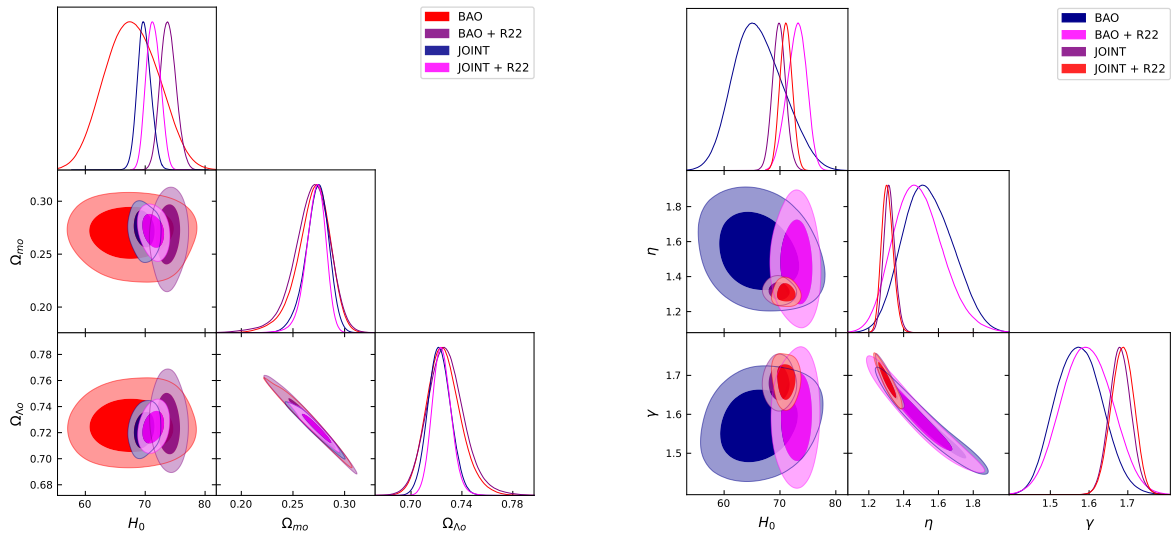

a) ΛCDM Model

b) LVDP Model

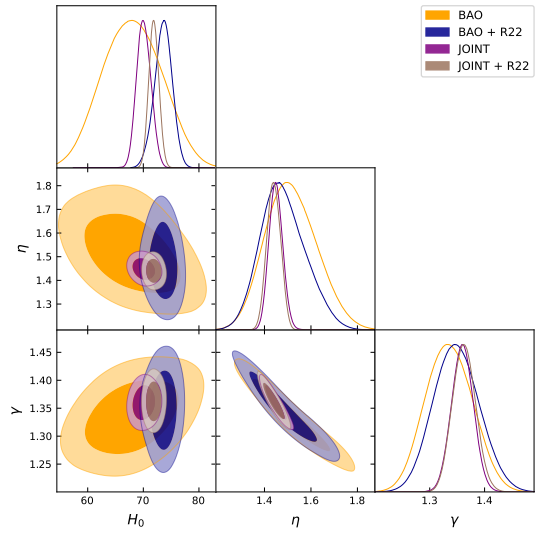

c) QVDP Model

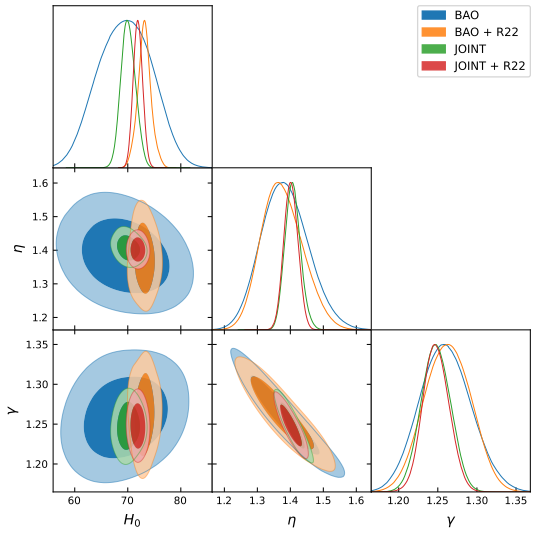

d) CVDP Model

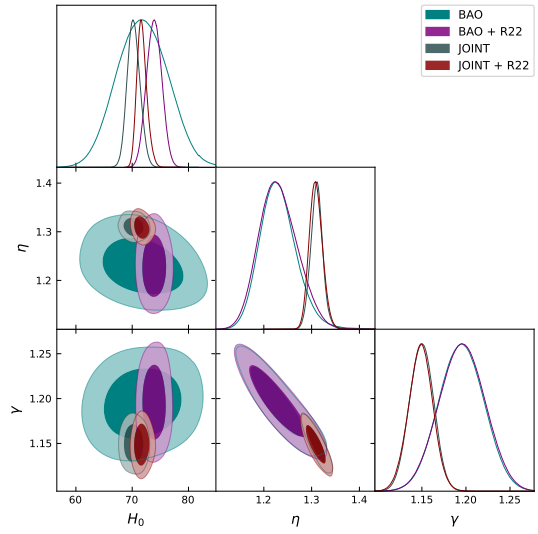

e) QUADP Model

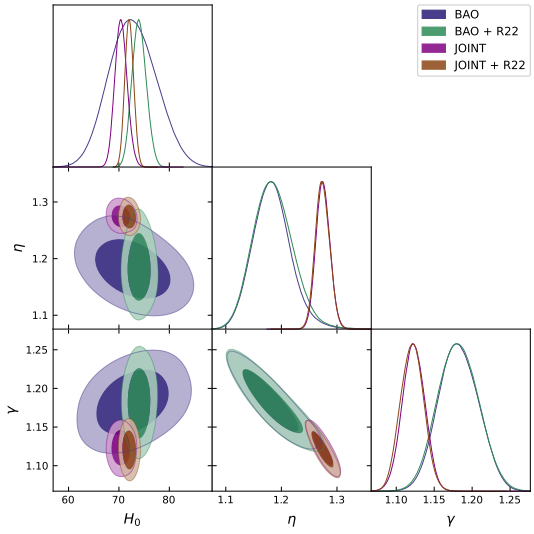

f) QUIDP Model

FIG. 3: The figure presents the posterior distribution for various observational data measurements with the ΛCDM, LVDP, QVDP, CVDP, QUADP, and QUIDP Models indicating 1 σ and 2σ confidence intervals.

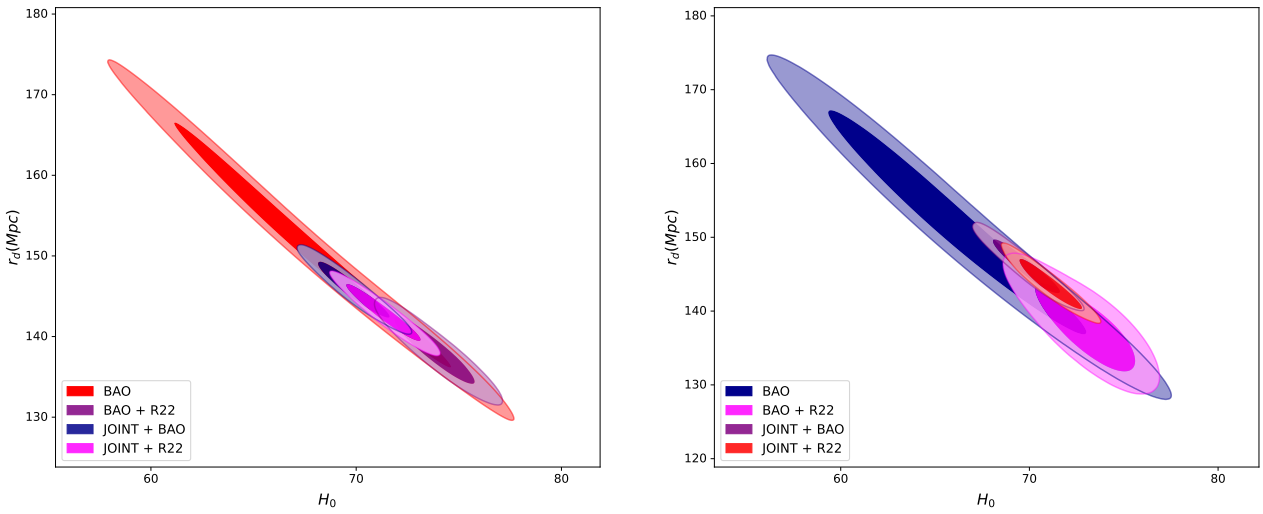

a) ΛCDM Model

b) LVDP Model

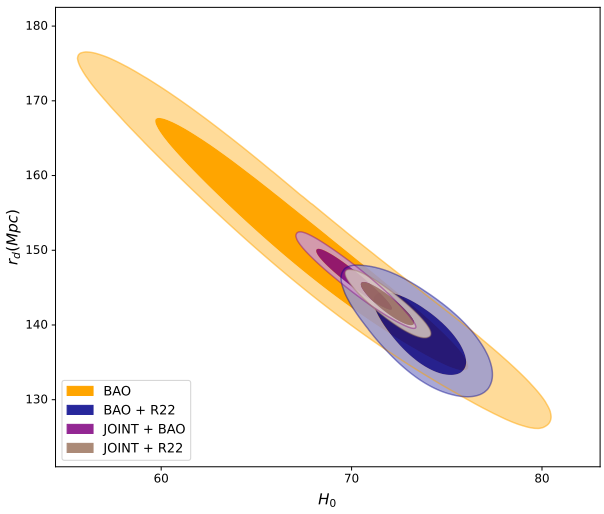

c) QVDP Model

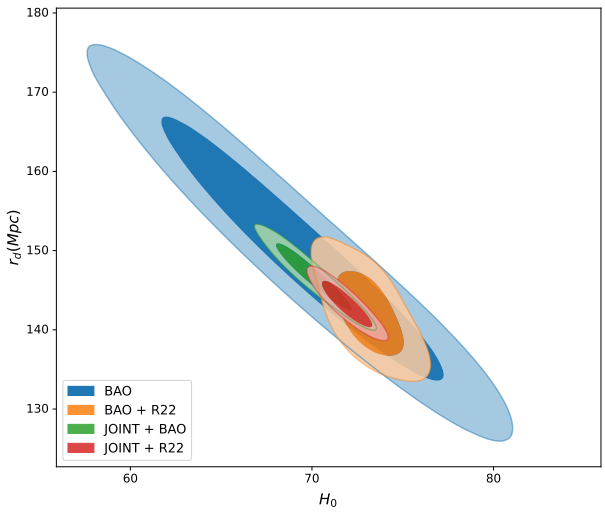

d) CVDP Model

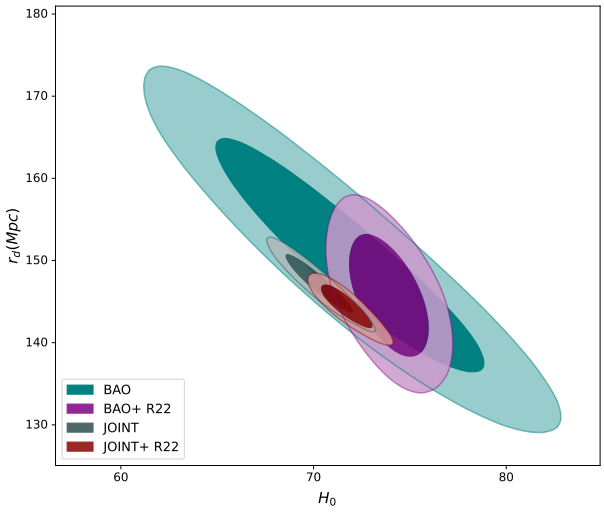

e) QUADP Model

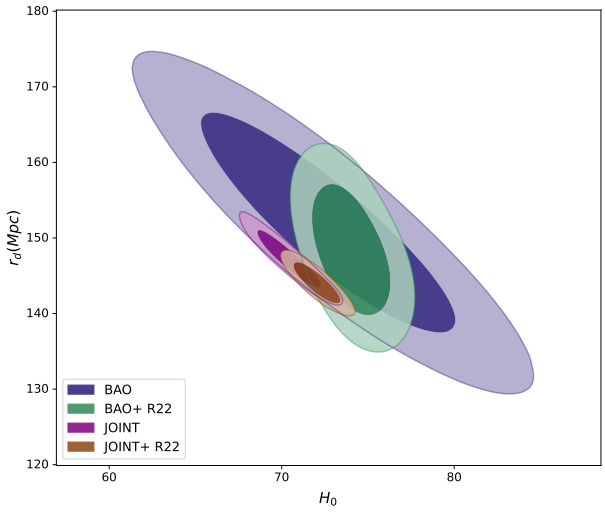

f) QUIDP Model

FIG. 4: The figure displays the posterior distribution for various observational data measurements in the r_d vs. H_0 contour plane of the ΛCDM, LVDP, QVDP, CVDP, QUADP, and QUIDP Models, indicating 1 σ and 2σ confidence intervals.

MCMC Results						
Model	Parameters	Priors	BAO	BA0 + R22	JOINT	JOINT + R22
ΛCDM Model	H_0	[50,100]	$70.256^{\pm 9.206}_{\pm 5.502}$	$73.798^{\pm 2.543}_{\pm 1.315}$	$69.837^{\pm 2.478}_{\pm 1.204}$	$71.508^{\pm 1.614}_{\pm 0.882}$
	Ω_{m0}	[0.,1.]	$0.270^{\pm 0.033}_{\pm 0.013}$	$0.268^{\pm 0.043}_{\pm 0.016}$	$0.274^{\pm 0.021}_{\pm 0.009}$	$0.270^{\pm 0.022}_{\pm 0.009678}$
	$\Omega_{\Lambda 0}$	[0.,1.]	$0.725^{\pm 0.019}_{\pm 0.011}$	$0.727^{\pm 0.024379}_{\pm 0.013}$	$0.721607^{\pm 0.015585}_{\pm 0.007421}$	$0.724854^{\pm 0.016354}_{\pm 0.007274}$
	r_d(Mpc)	[100.,200.]	$145.807^{\pm 13.994}_{\pm 9.060}$	$138.345^{\pm 4.939}_{\pm 2.451}$	$145.811^{\pm 4.545}_{\pm 2.347}$	$142.591^{\pm 3.951}_{\pm 1.850}$
	r_d/r_{fid}	[0.9,1.1]	$0.970^{\pm 0.068}_{\pm 0.055}$	$0.930^{\pm 0.028}_{\pm 0.021}$	$0.974^{\pm 0.057}_{\pm 0.033}$	$0.947^{\pm 0.043}_{\pm 0.028}$
LVDP Model	H_0	[50,100]	$66.482^{\pm 7.523}_{\pm 4.327}$	$73.399^{\pm 2.121}_{\pm 1.233}$	$69.843^{\pm 2.309}_{\pm 1.201}$	$71.089^{\pm 1.860}_{\pm 1.098}$
	η	[1.,2.]	$1.543^{\pm 0.235}_{\pm 0.155}$	$1.505^{\pm 0.238}_{\pm 0.135}$	$1.317^{\pm 0.059}_{\pm 0.029}$	$1.306^{\pm 0.057}_{\pm 0.032}$
	γ	[1.,2.]	$1.569^{\pm 0.091}_{\pm 0.060}$	$1.584^{\pm 0.095406}_{\pm 0.049}$	$1.680^{\pm 0.052}_{\pm 0.026}$	$1.686^{\pm 0.059}_{\pm 0.027}$
	r_d[Mpc]	[100.,200.]	$150.937^{\pm 16.766}_{\pm 10.441}$	$136.635^{\pm 4.733}_{\pm 2.578}$	$145.943^{\pm 4.424}_{\pm 2.304}$	$143.601^{\pm 3.924}_{\pm 2.166}$
	r_d/r_{fid}	[0.9,1.1]	$0.998^{\pm 0.089}_{\pm 0.061}$	$0.924^{\pm 0.024}_{\pm 0.019}$	$0.973^{\pm 0.056}_{\pm 0.030}$	$0.970^{\pm 0.062}_{\pm 0.040}$
QVDP Model	H_0	[50,100]	$68.017^{\pm 9.000}_{\pm 5.502}$	$73.595^{\pm 3.369}_{\pm 1.429}$	$70.087223^{\pm 2.27}_{\pm 1.264}$	$71.888^{\pm 1.603}_{\pm 0.827}$
	η	[1.,1.8]	$1.513^{\pm 0.180}_{\pm 0.103}$	$1.479^{\pm 0.174}_{\pm 0.092}$	$1.448^{\pm 0.050}_{\pm 0.029}$	$1.439^{\pm 0.054}_{\pm 0.026}$
	γ	[1.4,1.9]	$1.335^{\pm 0.069}_{\pm 0.044}$	$1.348^{\pm 0.071}_{\pm 0.042}$	$1.359^{\pm 0.037}_{\pm 0.018}$	$1.362^{\pm 0.035}_{\pm 0.020}$
	r_d[Mpc]	[100.,200.]	$150.225^{\pm 15.858}_{\pm 11.258}$	$138.891^{\pm 5.163}_{\pm 3.466}$	$146.210^{\pm 5.011}_{\pm 2.671}$	$142.833^{\pm 3.171}_{\pm 1.905}$
	r_d/r_{fid}	[0.9,1.1]	$0.995^{\pm 0.091}_{\pm 0.075}$	$0.930^{\pm 0.029}_{\pm 0.022}$	$0.973^{\pm 0.056}_{\pm 0.032}$	$0.952^{\pm 0.049}_{\pm 0.029}$
CVDP Model	H_0	[50,100]	$69.506^{\pm 8.430}_{\pm 5.350}$	$73.142^{\pm 2.735}_{\pm 1.084}$	$70.088^{\pm 2.347}_{\pm 1.290}$	$71.911^{\pm 1.579}_{\pm 0.855}$
	η	[1.,1.6]	$1.382^{\pm 0.118}_{\pm 0.069}$	$1.375^{\pm 0.102}_{\pm 0.059}$	$1.407^{\pm 0.040}_{\pm 0.023}$	$1.401^{\pm 0.036}_{\pm 0.020}$
	γ	[1.,2.]	$1.259^{\pm 0.060}_{\pm 0.032}$	$1.262^{\pm 0.050}_{\pm 0.029}$	$1.247^{\pm 0.034}_{\pm 0.018}$	$1.247^{\pm 0.030}_{\pm 0.015}$
	r_d[Mpc]	[100.,200.]	$149.861^{\pm 15.937}_{\pm 11.055}$	$142.044^{\pm 6.072}_{\pm 3.263}$	$146.722^{\pm 5.262}_{\pm 2.920}$	$143.240^{\pm 3.419}_{\pm 1.733}$
	r_d/r_{fid}	[0.9,1.1]	$0.992^{\pm 0.087}_{\pm 0.068}$	$0.942^{\pm 0.038}_{\pm 0.025}$	$0.973^{\pm 0.062}_{\pm 0.028}$	$0.952^{\pm 0.048}_{\pm 0.026}$
QUADP Model	H_0	[50,100]	$71.809^{\pm 7.774}_{\pm 4.373}$	$73.903^{\pm 2.419}_{\pm 1.204}$	$70.257^{\pm 1.834241}_{\pm 1.023}$	$71.716^{\pm 1.404}_{\pm 0.867}$
	η	[1.,1.45]	$1.229^{\pm 0.064}_{\pm 0.036}$	$1.229^{\pm 0.063}_{\pm 0.035}$	$1.310^{\pm 0.024}_{\pm 0.012}$	$1.308^{\pm 0.024}_{\pm 0.014}$
	γ	[1.,1.5]	$1.194^{\pm 0.044}_{\pm 0.026}$	$1.195^{\pm 0.047}_{\pm 0.024}$	$1.149^{\pm 0.024}_{\pm 0.013}$	$1.148^{\pm 0.027}_{\pm 0.012}$
	r_d (Mpc)	[100.,200.]	$150.404^{\pm 15.311}_{\pm 9.337}$	$145.723^{\pm 8.062}_{\pm 4.129}$	$147.192^{\pm 4.304}_{\pm 2.253}$	$144.383^{\pm 3.597}_{\pm 1.707}$
	r_d/r_{fid}	[0.9,1.1]	$1.001^{\pm 0.093}_{\pm 0.061}$	$0.971^{\pm 0.068}_{\pm 0.038}$	$0.973^{\pm 0.053}_{\pm 0.031}$	$0.956^{\pm 0.046}_{\pm 0.025}$
QUIDP Model	H_0	[50,100]	$72.717^{\pm 8.174}_{\pm 4.717}$	$74.018^{\pm 2.524}_{\pm 1.370}$	$70.420^{\pm 2.148}_{\pm 1.243}$	$72.049^{\pm 1.519}_{\pm 0.838}$
	η	[1.,1.4]	$1.182^{\pm 0.059}_{\pm 0.033}$	$1.184^{\pm 0.056}_{\pm 0.034}$	$1.274^{\pm 0.022}_{\pm 0.011}$	$1.273^{\pm 0.021}_{\pm 0.011}$
	γ	[1.,1.5]	$1.182^{\pm 0.046}_{\pm 0.023}$	$1.181^{\pm 0.048}_{\pm 0.025}$	$1.122^{\pm 0.029}_{\pm 0.013}$	$1.120^{\pm 0.027763}_{\pm 0.014}$
	r_d (Mpc)	[100.,200.]	$151.765^{\pm 15.340}_{\pm 9.674}$	$148.365^{\pm 9.457}_{\pm 4.899}$	$147.185^{\pm 4.439}_{\pm 2.348}$	$144.031^{\pm 3.256}_{\pm 1.604}$
	r_d/r_{fid}	[0.9,1.1]	$1.001^{\pm 0.093}_{\pm 0.059}$	$0.983^{\pm 0.074}_{\pm 0.042}$	$0.975^{\pm 0.062}_{\pm 0.030}$	$0.951^{\pm 0.045}_{\pm 0.028}$

TABLE I: Constraints at 95% CL on the cosmological parameters for ΛCDM, LVDP, QVDP, CVDP, QUADP and QUIDP Models

Additionally, despite efforts to minimize correlations within our selected data subset, intrinsic correlations may persist. To simulate such correlations, we introduce non-diagonal elements into the covariance matrix, maintaining symmetry. These elements are randomly assigned with magnitudes based on the product of corresponding data point errors, scaled by 0.5, effectively covering about 55% of the BAO dataset. While non-diagonal elements' positions are random, their magnitudes reflect expected correlations, enhancing dataset representation. Fig 2a, 2b, 2c, 2d, 2e, and 2f display posterior distributions for ΛCDM, LVDP, QVDP, CVDP, QAVDP, and QIVDP respectively, with and without a test random covariance matrix of fourteen components. These findings suggest a limited influence on model posterior distributions. In Figs. 3a, 3b, 3c, 3d, 3e, and 3f, the 68% and 95% confidence levels depict the posterior distribution of key cosmological parameters in the ΛCDM, LVDP, QVDP, CVDP, QUADP, and QUIDP models. The optimal values of each model are represented in Table I. By observing the H_0 values presented in Table I for each model, one can notice that when the R22 prior is incorporated into the Joint dataset, the optimal fitting value for H_0 deviates from the result in [85] but closely aligns with measurements from the SNIe sample in [84]. In the absence of R22 priors with the Joint dataset, the estimated H_0 aligns more closely with the value obtained in [85] in each model. For the Standard ΛCDM model, the determined values for the matter density, referred to as Ω_{m0}, and the dark energy density, represented by $\Omega_{\Lambda 0}$, seem to be relatively lower compared to the documented values in [85]. In the context of the Baryon Acoustic Oscillations (BAO) scale, it is defined by the cosmic sound horizon imprinted in the cosmic microwave background during the drag epoch, denoted as z_d. This epoch marks the separation of baryons and photons. The BAO scale, represented by r_d, is determined by the integral of the ratio of the speed of sound (c_s) to the Hubble parameter (H) over the redshift range from z_d to infinity. The speed of sound, c_s, is given by $\sqrt{\frac{\delta p_\gamma}{\delta\rho_B+\delta\rho_\gamma}}$, where δp_γ is the pressure perturbation in photons, and $\delta\rho_B$ and $\delta\rho_\gamma$ are perturbations in the baryon and photon energy densities, respectively. This expression is further simplified to $\frac{1}{\sqrt{3(1+R)}}$, with R defined as the ratio of baryon density perturbation to photon density perturbation ($R \equiv \frac{\delta\rho_B}{\delta\rho_\gamma} = \frac{3\rho_B}{4\rho_\gamma}$). Observational data from [85] provides the redshift at the drag epoch as $z_d = 1059.94 \pm 0.30$. Fig 4 illustrates the posterior distribution of the contour plane for $r_d - H_0$ in the ΛCDM model and each dark energy model obtained from different parameterizations. In Fig 4a, the BAO datasets estimate r_d as 145.807 ± 9.06 Mpc, consistent with [85]. When R22 prior is included exclusively, r_d becomes 138.345 ± 2.45 Mpc. For the Joint dataset, r_d is 145.811 ± 2.34 Mpc, aligning closely with [85]. Incorporating R22 into the comprehensive dataset results in r_d of 142.591 ± 1.49 Mpc, similar to [86]. Transitioning to the LVDP parameterization, Fig 4b showcases the contour plane of $r_d - H_0$. In the case of BAO datasets, r_d is 150.225 ± 11.258 Mpc. When exclusively incorporating the R22 prior into BAO datasets, the sound horizon at the drag epoch is 138.891 ± 3.466 Mpc. For the Joint dataset, r_d is 145.943 ± 2.30 Mpc, closely resembling [85]. Integrating the R22 prior into the comprehensive dataset yields $r_d = 143.601 \pm 2.166$ Mpc, akin to the results in [86]. Moving to the QVDP parameterization (Fig 4c), the contour plane of $r_d - H_0$ is depicted. BAO datasets estimate r_d as 150.225 ± 11.258 Mpc. Introducing the R22 before BAO datasets results in a sound horizon of 138.891 ± 3.466 Mpc. For the Joint dataset, r_d is 146.210 ± 2.671 Mpc, resembling [85]. Incorporating the R22 prior into the complete dataset yields $r_d = 142.833 \pm 1.905$ Mpc, in agreement with [86]. Shifting our focus to the CVDP parameterization Fig 4d, the contour plane of $r_d - H_0$ is illustrated. BAO datasets estimate r_d as 149.861 ± 11.055 Mpc. Introducing the R22 before BAO datasets alone results in a sound horizon of 142.044 ± 3.263 Mpc. For the Joint dataset, r_d is 146.722 ± 2.920 Mpc, aligning with [85]. Incorporating the R22 prior into the full dataset yields $r_d = 143.240 \pm 1.733$ Mpc, showing proximity to the outcomes in [86]. Turning our attention to the QUADP parameterization Fig 4e, the contour plane of $r_d - H_0$ is shown. BAO datasets estimate r_d as 150.404 ± 9.377 Mpc. Introducing the R22 before BAO datasets alone yields a sound horizon of 145.723 ± 4.129 Mpc. For the Joint dataset, r_d is 147.192 ± 2.253 Mpc, closely resembling [85]. Incorporating the R22 prior into the full dataset results in $r_d = 144.383 \pm 1.707$ Mpc, showing proximity to the outcomes in [86]. Finally, Shifting the focus to the QUIDP parameterization Fig 4f, the contour plane of $r_d - H_0$ is depicted. BAO datasets estimate r_d as 151.765 ± 9.674 Mpc. Introducing the R22 prior to BAO datasets alone yields a sound horizon of 148.365 ± 4.899 Mpc. For the Joint dataset, r_d is 147.185 ± 2.348 Mpc, closely resembling [85]. Incorporating the R22 prior into the full dataset results in $r_d = 144.031 \pm 1.604$ Mpc, showing proximity to the outcomes in [86]. The r_d values obtained from the joint dataset in the ΛCDM, LVDP, QVDP, CVDP, QUADP, and QUIDP models exhibit close agreement with the estimates provided by Planck and SDSS. [87] reports that by employing Binning and Gaussian methods to

combine measurements of 2D BAO and SNIa data, the values of the absolute BAO scale range from 141.45 Mpc to $r_d \leq 159.44$Mpc (Binning) and 143.35 Mpc to $r_d \leq 161.59$Mpc (Gaussian). These findings highlight a clear discrepancy between early and late-time observational measurements, analogous to the H_0 tension. It is noteworthy that our results critically depend the range of priors for r_d and H_0, for r_d, tighter priors are favored because they constrain its range, influencing the estimation of H_0. If r_d is tightly constrained, H_0 must adjust to maintain consistency with the data, affecting the $r_d - H_0$ parameter space. The choice of prior for r_d can have as much impact on parameter estimation as a tight prior for H_0, demonstrating a significant correlation between r_d and H_0. Conversely, a tight prior on H_0 restricts its values, dominating the results even if r_d has a broad interval. In our quest to compare various cosmological models, we employ two widely used criteria, namely the Akaike Information Criterion (AIC) [88] and the Bayesian Information Criterion (BIC) [89]. The AIC is given by the formula: $\text{AIC} = -2\ln(\mathcal{L}_{\max}) + 2k + \frac{2k(2k+1)}{N_{\text{tot}}-k-1}$ Here, $\mathcal{L}_{\max}$ represents the maximum likelihood of the data, N_{tot} is the total number of data points (in our case, $N_{\text{tot}} = 299$), and k is the number of parameters. For sufficiently large N_{tot}, the expression simplifies to the standard form: $\text{AIC} \approx -2\ln(\mathcal{L}_{\max}) + 2k$. The Bayesian Information Criterion is defined as $\text{BIC} = -2\ln(\mathcal{L}_{\max}) + k\ln(N_{\text{tot}})$ By applying these criteria to the standard ΛCDM, LVDP, QVDP, CVDP, QUADP and QUIDP models, we obtain AIC values of [264.53, 275.62, 271.48, 271.08, 274.66, 278.72] and BIC values of [264.53, 275.85, 271.71, 271.30, 274.88, 278.94] for the respective models. While the ΛCDM model exhibits the best fit due to the lowest AIC, it is noteworthy that our AIC and BIC values collectively lend substantial support to all the tested models. Consequently, none of the models can be conclusively ruled out based on the current dataset. This underscores the robustness of our findings and the validity of the cosmological models under consideration. When comparing the LVDP, QVDP, CVDP, QUADP, and QUIDP models to ΛCDM, it is important to note that ΛCDM is nested within both proposed extensions, with a difference of 5 degrees of freedom. This characteristic enables the application of standard statistical tests. The assessment involves utilizing the reduced chi-square statistic, denoted as $\chi^2_{\text{red}} = \chi^2/\text{Dof}$, where Dof represents the degrees of freedom of the model, and χ^2 signifies the weighted sum of squared deviations. Under an equal number of runs for the three models, the reduced chi-square statistic closely approximates 1, as shown by the values: $\left(\frac{\chi^2}{Dof_{\Lambda CDM}}, \frac{\chi^2}{Dof_{LVDP}}, \frac{\chi^2}{Dof_{QVDP}}, \frac{\chi^2}{Dof_{CVDP}}, \frac{\chi^2}{Dof_{QUADP}}, \frac{\chi^2}{Dof_{QUIDP}}\right) \approx \{0.961646, 0.955499, 0.943959, 0.955646, 0.952016, 0.966625\}$. This comparative analysis provides insights into the goodness of fit for each model, where values close to 1 suggest a reasonable fit to the data.

V. CONCLUSION

In our investigation, we adopted a parametrization scheme for the Hubble parameter, yielding cosmological models with varying deceleration parameter profiles (LVDP, QVDP, CVDP, QUADP, and QUIDP). These models exhibit distinct behaviors in the Universe's late-time evolution. By constraining parameters such as η and γ, we aligned these models with observational data, offering insights into the Universe's expansion history and its transition to an accelerating phase. We selected 24 Baryon Acoustic Oscillation (BAO) data points from a larger set of 333 to ensure independence and minimize intrinsic errors in the posterior distribution. We introduced random correlations to the covariance matrix, confirming that these additions do not significantly alter the derived cosmological parameters. Alongside BAO data, we incorporated low-redshift data: 33 Hubble Measurements from Cosmic Chronometers, 40 data points from Type Ia supernovae, 24 points from the Hubble diagram for quasars, and 162 points from Gamma-Ray Bursts. This comprehensive dataset, along with the latest Hubble constant measurement by R22, enabled us to analyze the sensitivity of the Hubble constant and sound horizon within the Pacif parametrization. We treated r_d as a free parameter rather than imposing a prior constraint from CMB measurements. Our findings for the Hubble constant H_0 and sound horizon r_d are as follows: - ΛCDM: $H_0 = 69.84 \pm 1.20$ km/s/Mpc, $r_d = 145.81 \pm 2.35$ Mpc - LVDP: $H_0 = 69.84 \pm 1.20$ km/s/Mpc, $r_d = 145.94 \pm 2.30$ Mpc - QVDP: $H_0 = 70.09 \pm 1.26$ km/s/Mpc, $r_d = 146.21 \pm 2.67$ Mpc - CVDP: $H_0 = 70.09 \pm 1.29$ km/s/Mpc, $r_d = 146.72 \pm 2.92$ Mpc - QUADP: $H_0 = 70.26 \pm 1.02$ km/s/Mpc, $r_d = 147.19 \pm 2.25$ Mpc - QUIDP: $H_0 = 70.42 \pm 1.24$ km/s/Mpc, $r_d = 147.19 \pm 2.35$ Mpc Remarkably, these H_0 and r_d values from low-redshift measurements are consistent with early Planck estimates. Using the Akaike Information Criterion (AIC) and the Bayesian Information Criterion (BIC), we evaluated the models' comparative performance. While the ΛCDM model showed the best fit with the lowest AIC value, all models received substantial support from the AIC and BIC, indicating their validity. None

of the models can be definitively ruled out based on the current dataset. The reduced chi-square statistics approximating 1 for each model suggest a reasonable fit to the data. In conclusion, our investigation into Pacif parametrization models demonstrates their efficacy in capturing late-time cosmological evolution and addressing existing tensions. By refining constraints through non-diagonal elements in the covariance matrix and leveraging diverse datasets spanning various redshifts, we achieve robust H_0 and r_d estimates. Our findings, consistent with Planck CMB results, affirm the viability of Pacif parametrization models, offering valuable insights for advancing cosmological understanding amidst evolving observational landscapes.

[1] D. H. Weinberg, M. J. Mortonson, D. J. Eisenstein, C. Hirata, A. G. Riess, and E. Rozo, "Observational probes of cosmic acceleration," *Physics reports*, vol. 530, no. 2, pp. 87–255, 2013.

[2] A. G. Riess, A. V. Filippenko, P. Challis, A. Clocchiatti, A. Diercks, P. M. Garnavich, R. L. Gilliland, C. J. Hogan, S. Jha, R. P. Kirshner, *et al.*, "Observational evidence from supernovae for an accelerating universe and a cosmological constant," *The astronomical journal*, vol. 116, no. 3, p. 1009, 1998.

[3] S. Perlmutter and B. P. Schmidt, "Measuring cosmology with supernovae," *Supernovae and Gamma-Ray Bursters*, pp. 195–217, 2003.

[4] S. Perlmutter, G. Aldering, G. Goldhaber, R. A. Knop, P. Nugent, P. G. Castro, S. Deustua, S. Fabbro, A. Goobar, D. E. Groom, *et al.*, "Measurements of ω and λ from 42 high-redshift supernovae," *The Astrophysical Journal*, vol. 517, no. 2, p. 565, 1999.

[5] S. Weinberg, *Cosmology*. OUP Oxford, 2008.

[6] J. A. Frieman, M. S. Turner, and D. Huterer, "Dark energy and the accelerating universe," *Annu. Rev. Astron. Astrophys.*, vol. 46, pp. 385–432, 2008.

[7] P. J. E. Peebles and B. Ratra, "The cosmological constant and dark energy," *Reviews of modern physics*, vol. 75, no. 2, p. 559, 2003.

[8] D. N. Spergel, L. Verde, H. V. Peiris, E. Komatsu, M. Nolta, C. L. Bennett, M. Halpern, G. Hinshaw, N. Jarosik, A. Kogut, *et al.*, "First-year wilkinson microwave anisotropy probe (wmap)* observations: determination of cosmological parameters," *The Astrophysical Journal Supplement Series*, vol. 148, no. 1, p. 175, 2003.

[9] N. Aghanim, Y. Akrami, M. Ashdown, J. Aumont, C. Baccigalupi, M. Ballardini, A. J. Banday, R. Barreiro, N. Bartolo, S. Basak, *et al.*, "Planck 2018 results-vi. cosmological parameters," *Astronomy & Astrophysics*, vol. 641, p. A6, 2020.

[10] S. Carroll, "The cosmological constant, living riviews in relativity."

[11] E. V. Linder, "Mapping the cosmological expansion," *Reports on Progress in Physics*, vol. 71, no. 5, p. 056901, 2008.

[12] I. Zlatev, L. Wang, and P. J. Steinhardt, "Quintessence, cosmic coincidence, and the cosmological constant," *Physical Review Letters*, vol. 82, no. 5, p. 896, 1999.

[13] A. Iqbal, J. Prasad, T. Souradeep, and M. A. Malik, "Joint planck and wmap assessment of low cmb multipoles," *Journal of Cosmology and Astroparticle Physics*, vol. 2015, no. 06, p. 014, 2015.

[14] C.-H. Chuang, F. Prada, F. Beutler, D. J. Eisenstein, S. Escoffier, S. Ho, J.-P. Kneib, M. Manera, S. E. Nuza, D. J. Schlegel, *et al.*, "The clustering of galaxies in the sdss-iii baryon oscillation spectroscopic survey: single-probe measurements from cmass and lowz anisotropic galaxy clustering," *arXiv preprint arXiv:1312.4889*, 2013.

[15] O. Farooq, F. R. Madiyar, S. Crandall, and B. Ratra, "Hubble parameter measurement constraints on the redshift of the deceleration–acceleration transition, dynamical dark energy, and space curvature," *The Astrophysical Journal*, vol. 835, no. 1, p. 26, 2017.

[16] M. Li, X.-D. Li, S. Wang, and Y. Wang, "Dark energy," *Communications in theoretical physics*, vol. 56, no. 3, p. 525, 2011.

[17] M. Li, X.-D. Li, S. Wang, and Y. Wang, "Dark energy: A brief review," *Frontiers of Physics*, vol. 8, pp. 828–846, 2013.

[18] L. Izzo, O. Luongo, and S. Capozziello, "Cosmographic applications of gamma ray bursts," *arXiv preprint arXiv:1011.1151*, 2010.

[19] A. Aviles, C. Gruber, O. Luongo, and H. Quevedo, "Cosmography and constraints on the equation of state of the universe in various parametrizations," *Physical Review D*, vol. 86, no. 12, p. 123516, 2012.

[20] C. Gruber and O. Luongo, "Cosmographic analysis of the equation of state of the universe through padé approximations," *Physical Review D*, vol. 89, no. 10, p. 103506, 2014.

[21] A. Aviles, A. Bravetti, S. Capozziello, and O. Luongo, "Precision cosmology with padé rational approximations: Theoretical predictions versus observational limits," *Physical Review D*, vol. 90, no. 4, p. 043531, 2014.

[22] P. K. Dunsby and O. Luongo, "On the theory and applications of modern cosmography," *International Journal of Geometric Methods in Modern Physics*, vol. 13, no. 03, p. 1630002, 2016.

[23] A. Aviles, J. Klapp, and O. Luongo, "Toward unbiased estimations of the statefinder parameters," *Physics of the dark universe*, vol. 17, pp. 25–37, 2017.

[24] S. Capozziello, R. D'Agostino, and O. Luongo, "Cosmographic analysis with chebyshev polynomials," *Monthly Notices of the Royal Astronomical Society*, vol. 476, no. 3, pp. 3924–3938, 2018.

[25] S. Capozziello, R. D'Agostino, and O. Luongo, "High-redshift cosmography: auxiliary variables versus padé polynomials," *Monthly Notices of the Royal Astronomical*

Society, vol. 494, no. 2, pp. 2576–2590, 2020.

[26] O. Luongo and M. Muccino, "Kinematic constraints beyond $z \simeq 0$ using calibrated GRB correlations," *Astron. Astrophys.*, vol. 641, p. A174, 2020.

[27] O. Luongo and M. Muccino, "Model-independent calibrations of gamma-ray bursts using machine learning," *Monthly Notices of the Royal Astronomical Society*, vol. 503, no. 3, pp. 4581–4600, 2021.

[28] S. Capozziello, P. K. Dunsby, and O. Luongo, "Model-independent reconstruction of cosmological accelerated–decelerated phase," *Monthly Notices of the Royal Astronomical Society*, vol. 509, no. 4, pp. 5399–5415, 2022.

[29] A. C. Alfano, C. Cafaro, S. Capozziello, and O. Luongo, "Dark energy–matter equivalence by the evolution of cosmic equation of state," *Physics of the Dark Universe*, vol. 42, p. 101298, 2023.

[30] O. Luongo and M. Muccino, "Model independent cosmographic constraints from desi 2024," *arXiv preprint arXiv:2404.07070*, 2024.

[31] E. J. Copeland, M. Sami, and S. Tsujikawa, "Dynamics of dark energy," *International Journal of Modern Physics D*, vol. 15, no. 11, pp. 1753–1935, 2006.

[32] B. Kazuharu, S. Capozziello, S. D. Odintsov, *et al.*, "Dark energy cosmology: the equivalent description via different theoretical models and cosmography tests," *ASTROPHYSICS AND SPACE SCIENCE*, vol. 342, pp. 155–228, 2012.

[33] A. Bouali, H. Chaudhary, A. Mehrotra, and S. Pacif, "Model-independent study for a quintessence model of dark energy: Analysis and observational constraints," *arXiv preprint arXiv:2304.02652*, 2023.

[34] S. K. J. Pacif, "Dark energy models from a parametrization of h: a comprehensive analysis and observational constraints," *The European Physical Journal Plus*, vol. 135, no. 10, pp. 1–34, 2020.

[35] M. Khurana, H. Chaudhary, S. Mumtaz, S. Pacif, and G. Mustafa, "Cosmic evolution in f (q, t) gravity: Exploring a higher-order time-dependent function of deceleration parameter with observational constraints," *Physics of the Dark Universe*, vol. 43, p. 101408, 2024.

[36] L. Berezhiani, J. Khoury, and J. Wang, "Universe without dark energy: Cosmic acceleration from dark matter-baryon interactions," *Physical Review D*, vol. 95, no. 12, p. 123530, 2017.

[37] M. K. Sharma, S. K. J. Pacif, G. Yergaliyeva, and K. Yesmakhanova, "The oscillatory universe, phantom crossing and the hubble tension," *Annals of Physics*, vol. 454, p. 169345, 2023.

[38] H. Chaudhary, A. Bouali, U. Debnath, T. Roy, and G. Mustafa, "Constraints on the parameterized deceleration parameter in frw universe," *Physica Scripta*, vol. 98, no. 9, p. 095006, 2023.

[39] A. Bouali, H. Chaudhary, U. Debnath, A. Sardar, and G. Mustafa, "Data analysis of three parameter models of deceleration parameter in flrw universe," *The European Physical Journal Plus*, vol. 138, no. 9, p. 816, 2023.

[40] A. Bouali, B. Shukla, H. Chaudhary, R. K. Tiwari, M. Samar, and G. Mustafa, "Cosmological tests of parametrization q= α- β h in f (q) flrw cosmology," *International Journal of Geometric Methods in Modern Physics*, vol. 20, no. 09, p. 2350152, 2023.

[41] A. Bouali, H. Chaudhary, S. Mumtaz, G. Mustafa, and S. Maurya, "Observational constraining study of new deceleration parameters in frw universe," *Fortschritte der Physik*, vol. 71, no. 10-11, p. 2300033, 2023.

[42] B. K. Shukla, A. Bouali, H. Chaudhary, R. K. Tiwari, and M. S. Martín, "Cosmographic studies of q= α- β h parametrization in $f(t)$ framework," *International Journal of Geometric Methods in Modern Physics*, vol. 20, no. 14, pp. 2450007–8, 2023.

[43] H. Chaudhary, A. Kaushik, and A. Kohli, "Cosmological test of $\sigma\theta$ as function of scale factor in f (r, t) framework," *New Astronomy*, vol. 103, p. 102044, 2023.

[44] D. Arora, H. Chaudhary, S. K. J. Pacif, and G. Mustafa, "Diagnostic and comparative analysis of dark energy models with q (z) parametrizations," *The European Physical Journal Plus*, vol. 139, no. 5, pp. 1–20, 2024.

[45] B. Shukla, D. Sofuoğlu, H. Chaudhary, F. Atamurotov, and G. Mustafa, "Cosmic evolution in $f(q,t)$ gravity with observational constraints: A comparative analysis with λcdm," *Journal of High Energy Astrophysics*, 2024.

[46] H. Chaudhary, A. Bouali, H. Duru, E. Gudekli, and G. Mustafa, "Exploring the deceleration parameter in $f(t)$ gravity: A comprehensive analysis using parametrization techniques and observational data," *International Journal of Geometric Methods in Modern Physics*, 2024.

[47] H. Chaudhary, S. Mumtaz, A. Bouali, U. Debnath, and G. Mustafa, "Parametrization of the deceleration parameter in a flat flrw universe: constraints and comparative analysis with the λ cdm paradigm," *General Relativity and Gravitation*, vol. 55, no. 11, p. 133, 2023.

[48] H. Chaudhary, A. Bouali, N. U. Molla, U. Debnath, and G. Mustafa, "Cosmological tests of $f(r,g,t)$ dark energy model in frw universe," *The European Physical Journal C*, vol. 83, no. 10, p. 918, 2023.

[49] B. K. Shukla, A. Bouali, H. Chaudhary, R. K. Tiwari, and M. S. Martín, "Cosmographic studies of q= α- β h parametrization in f (t) framework," *International Journal of Geometric Methods in Modern Physics*, vol. 20, no. 14, pp. 2450007–8, 2023.

[50] M. Khurana, H. Chaudhary, S. Mumtaz, S. Pacif, and G. Mustafa, "Cosmic evolution in f (q, t) gravity: Exploring a higher-order time-dependent function of deceleration parameter with observational constraints," *Physics of the Dark Universe*, vol. 43, p. 101408, 2024.

[51] R. Kundu, U. Debnath, H. Chaudhary, and G. Mustafa, "Gravitational lensing and clues of $r\_\{d\}$ and $h\_\{0\}$ tension: Viscous modified chaplygin gas and variable modified chaplygin gas in loop quantum cosmology," *arXiv preprint arXiv:2402.07515*, 2024.

[52] G. N. Gadbail, H. Chaudhary, A. Bouali, and P. K. Sahoo, "Statistical and Observation Comparison of Weyl-Type $f(Q,T)$ Models with the ΛCDM Paradigm," 5 2023.

[53] S. Dahmani, H. Chaudhary, A. Bouali, S. K. J. Pacif, and T. Ouali, "Polytropic gas cosmology and late-time acceleration," *Available at SSRN 4697513*.

[54] H. Chaudhary, U. Debnath, T. Roy, S. Maity, and G. Mustafa, "Constraints on the parameters of modified chaplygin-jacobi and modified chaplygin-abel gases in $f(t)$ gravity model," *arXiv preprint arXiv:2307.14691*, 2023.

[55] S. Shekh, H. Chaudhary, A. Bouali, and A. Dixit, "Observational constraints on teleparallel effective equation of state," *General Relativity and Gravitation*, vol. 55, no. 8, p. 95, 2023.

[56] H. Chaudhary, N. U. Molla, M. Khurana, U. Debnath, and G. Mustafa, "Cosmological test of dark energy parameterizations in hořava–lifshitz gravity," *The European Physical Journal C*, vol. 84, no. 3, p. 223, 2024.

[57] H. Chaudhary, N. U. Molla, M. Khurana, U. Debnath, and G. Mustafa, "Cosmological test of dark energy parameterizations in hořava–lifshitz gravity," *The European Physical Journal C*, vol. 84, no. 3, p. 223, 2024.

[58] H. Chaudhary, U. Debnath, S. K. J. Pacif, N. U. Molla, G. Mustafa, and S. Maurya, "Investigating $\omega(z)$ parametrizations in horava-lifshitz gravity: Observational constraints with covariance matrix simulation," *arXiv preprint arXiv:2402.12324*, 2024.

[59] H. Chaudhary, U. Debnath, T. Roy, S. Maity, and G. Mustafa, "Constraints on the parameters of modified chaplygin-jacobi and modified chaplygin-abel gases in $f(t)$ gravity model," *arXiv preprint arXiv:2307.14691*, 2023.

[60] S. Maity, H. Chaudhary, U. Debnath, S. Maurya, and G. Mustafa, "Constraining cosmological parameters with viscous modified chaplygin gas and generalized cosmic chaplygin gas models in horava-lifshitz gravity: Utilizing late-time datasets," *arXiv preprint arXiv:2403.06286*, 2024.

[61] P. Mukherjee, U. Debnath, H. Chaudhary, and G. Mustafa, "The estimation of parameters of generalized cosmic chaplygin gas and viscous modified chaplygin gas and accretions around black hole in the background of einstein-aether gravity," *arXiv preprint arXiv:2405.15883*, 2024.

[62] U. Debnath, H. Chaudhary, N. U. Molla, S. Pacif, and G. Mustafa, "Dark energy model in einstein and horava-lifshitz gravity with a new parametrization of $\omega(z)$: Model comparison, analysis and observational constraint," *arXiv preprint arXiv:2405.15874*, 2024.

[63] D. Sofuoğlu, H. Baysal, and R. Tiwari, "Observational constraints on the cubic parametrization of the deceleration parameter in f (r, t) gravity," *The European Physical Journal Plus*, vol. 138, no. 6, pp. 1–14, 2023.

[64] V. Kalsariya and S. K. J. Pacif, "Cosmo-dynamics of dark energy models resulting from a parametrization of h in $f(q,t)$ gravity," *arXiv preprint arXiv:2304.09163*, 2023.

[65] A. J. Ross, L. Samushia, C. Howlett, W. J. Percival, A. Burden, and M. Manera, "The clustering of the sdss dr7 main galaxy sample–i. a 4 per cent distance measure at z= 0.15," *Monthly Notices of the Royal Astronomical Society*, vol. 449, no. 1, pp. 835–847, 2015.

[66] S. Alam, M. Ata, S. Bailey, F. Beutler, D. Bizyaev, J. A. Blazek, A. S. Bolton, J. R. Brownstein, A. Burden, C.-H. Chuang, *et al.*, "The clustering of galaxies in the completed sdss-iii baryon oscillation spectroscopic survey: cosmological analysis of the dr12 galaxy sample," *Monthly Notices of the Royal Astronomical Society*, vol. 470, no. 3, pp. 2617–2652, 2017.

[67] H. Gil-Marín, J. E. Bautista, R. Paviot, M. Vargas-Magaña, S. de La Torre, S. Fromenteau, S. Alam, S. Ávila, E. Burtin, C.-H. Chuang, *et al.*, "The completed sdss-iv extended baryon oscillation spectroscopic survey: measurement of the bao and growth rate of structure of the luminous red galaxy sample from the anisotropic power spectrum between redshifts 0.6 and 1.0," *Monthly Notices of the Royal Astronomical Society*, vol. 498, no. 2, pp. 2492–2531, 2020.

[68] A. Raichoor, A. De Mattia, A. J. Ross, C. Zhao, S. Alam, S. Avila, J. Bautista, J. Brinkmann, J. R. Brownstein, E. Burtin, *et al.*, "The completed sdss-iv extended baryon oscillation spectroscopic survey: large-scale structure catalogues and measurement of the isotropic bao between redshift 0.6 and 1.1 for the emission line galaxy sample," *Monthly Notices of the Royal Astronomical Society*, vol. 500, no. 3, pp. 3254–3274, 2021.

[69] J. Hou, A. G. Sánchez, A. J. Ross, A. Smith, R. Neveux, J. Bautista, E. Burtin, C. Zhao, R. Scoccimarro, K. S. Dawson, *et al.*, "The completed sdss-iv extended baryon oscillation spectroscopic survey: Bao and rsd measurements from anisotropic clustering analysis of the quasar sample in configuration space between redshift 0.8 and 2.2," *Monthly Notices of the Royal Astronomical Society*, vol. 500, no. 1, pp. 1201–1221, 2021.

[70] H. D. M. Des Bourboux, J. Rich, A. Font-Ribera, V. de Sainte Agathe, J. Farr, T. Etourneau, J.-M. Le Goff, A. Cuceu, C. Balland, J. E. Bautista, *et al.*, "The completed sdss-iv extended baryon oscillation spectroscopic survey: baryon acoustic oscillations with lyα forests," *The Astrophysical Journal*, vol. 901, no. 2, p. 153, 2020.

[71] T. Abbott, M. Aguena, S. Allam, A. Amon, F. Andrade-Oliveira, J. Asorey, S. Avila, G. Bernstein, E. Bertin, A. Brandao-Souza, *et al.*, "Dark energy survey year 3 results: A 2.7% measurement of baryon acoustic oscillation distance scale at redshift 0.835," *Physical Review D*, vol. 105, no. 4, p. 043512, 2022.

[72] S. Sridhar, Y.-S. Song, A. J. Ross, R. Zhou, J. A. Newman, C.-H. Chuang, R. Blum, E. Gaztanaga, M. Landriau, and F. Prada, "Clustering of lrgs in the decals dr8 footprint: Distance constraints from baryon acoustic oscillations using photometric redshifts," *The Astrophysical Journal*, vol. 904, no. 1, p. 69, 2020.

[73] F. Beutler, C. Blake, M. Colless, D. H. Jones, L. Staveley-Smith, L. Campbell, Q. Parker, W. Saunders, and F. Watson, "The 6df galaxy survey: baryon acoustic oscillations and the local hubble constant," *Monthly Notices of the Royal Astronomical Society*, vol. 416, no. 4, pp. 3017–3032, 2011.

[74] L. Kazantzidis and L. Perivolaropoulos, "Evolution of the f σ 8 tension with the planck 15/λcdm determination and

implications for modified gravity theories," *Physical Review D*, vol. 97, no. 10, p. 103503, 2018.

[75] W. Handley, M. Hobson, and A. Lasenby, "Polychord: nested sampling for cosmology," *Monthly Notices of the Royal Astronomical Society: Letters*, vol. 450, no. 1, pp. L61–L65, 2015.

[76] A. Lewis, "Getdist: a python package for analysing monte carlo samples," *arXiv preprint arXiv:1910.13970*, 2019.

[77] M. Moresco, "Raising the bar: new constraints on the hubble parameter with cosmic chronometers at z 2," *Monthly Notices of the Royal Astronomical Society: Letters*, vol. 450, no. 1, pp. L16–L20, 2015.

[78] M. Moresco, L. Pozzetti, A. Cimatti, R. Jimenez, C. Maraston, L. Verde, D. Thomas, A. Citro, R. Tojeiro, and D. Wilkinson, "A 6% measurement of the hubble parameter at z 0.45: direct evidence of the epoch of cosmic re-acceleration," *Journal of Cosmology and Astroparticle Physics*, vol. 2016, no. 05, pp. 014–014, 2016.

[79] M. Moresco, L. Verde, L. Pozzetti, R. Jimenez, and A. Cimatti, "New constraints on cosmological parameters and neutrino properties using the expansion rate of the universe to z 1.75," *Journal of Cosmology and Astroparticle Physics*, vol. 2012, no. 07, p. 053, 2012.

[80] M. Moresco, A. Cimatti, R. Jimenez, L. Pozzetti, G. Zamorani, M. Bolzonella, J. Dunlop, F. Lamareille, M. Mignoli, H. Pearce, *et al.*, "Improved constraints on the expansion rate of the universe up to z 1.1 from the spectroscopic evolution of cosmic chronometers," *Journal of Cosmology and Astroparticle Physics*, vol. 2012, no. 08, pp. 006–006, 2012.

[81] D. M. Scolnic, D. Jones, A. Rest, Y. Pan, R. Chornock, R. Foley, M. Huber, R. Kessler, G. Narayan, A. Riess, *et al.*, "The complete light-curve sample of spectroscopically confirmed sne ia from pan-starrs1 and cosmological constraints from the combined pantheon sample," *The Astrophysical Journal*, vol. 859, no. 2, p. 101, 2018.

[82] C. Roberts, K. Horne, A. O. Hodson, and A. D. Leggat, "Tests of λcdm and conformal gravity using grb and quasars as standard candles out to $z \sim 8$," *arXiv preprint arXiv:1711.10369*, 2017.

[83] M. Demianski, E. Piedipalumbo, D. Sawant, and L. Amati, "Cosmology with gamma-ray bursts-ii. cosmography challenges and cosmological scenarios for the accelerated universe," *Astronomy & Astrophysics*, vol. 598, p. A113, 2017.

[84] A. G. Riess, W. Yuan, L. M. Macri, D. Scolnic, D. Brout, S. Casertano, D. O. Jones, Y. Murakami, G. S. Anand, L. Breuval, *et al.*, "A comprehensive measurement of the local value of the hubble constant with 1 km s- 1 mpc- 1 uncertainty from the hubble space telescope and the sh0es team," *The Astrophysical journal letters*, vol. 934, no. 1, p. L7, 2022.

[85] P. Collaboration, N. Aghanim, Y. Akrami, M. Ashdown, J. Aumont, C. Baccigalupi, M. Ballardini, A. Banday, R. Barreiro, N. Bartolo, *et al.*, "Planck 2018 results. vi. cosmological parameters," 2020.

[86] L. Verde, J. L. Bernal, A. F. Heavens, and R. Jimenez, "The length of the low-redshift standard ruler," *Monthly Notices of the Royal Astronomical Society*, vol. 467, no. 1, pp. 731–736, 2017.

[87] T. Lemos, Ruchika, J. C. Carvalho, and J. Alcaniz, "Low-redshift estimates of the absolute scale of baryon acoustic oscillations," *The European Physical Journal C*, vol. 83, no. 6, p. 495, 2023.

[88] H. Akaike, "A new look at the statistical model identification," *IEEE transactions on automatic control*, vol. 19, no. 6, pp. 716–723, 1974.

[89] G. Schwarz, "Estimating the dimension of a model," *The annals of statistics*, pp. 461–464, 1978.